Journal of Catalysis **192,** 391–399 (2000)
doi:10.1006/jcat.2000.2857, available online at http://www.idealibrary.com on IDEAL®

Surface Science Based Microkinetic Analysis of Ammonia Synthesis over Ruthenium Catalysts

S. Dahl,* J. Sehested,† C. J. H. Jacobsen,† E. Törnqvist,† and I. Chorkendorff*,‡

*Center for Atomic-Scale Materials Physics (CAMP), Department of Physics, Technical University of Denmark, DK-2800 Lyngby, Denmark; †Haldor Topsøe Research Laboratories, DK-2800 Lyngby, Denmark; and ‡Interdisciplinary Research Center for Catalysis (ICAT), Technical University of Denmark, DK-2800 Lyngby, Denmark
E-mail: sordahl@fysik.dtu.dk

Received November 1, 1999; revised February 15, 2000; accepted February 16, 2000

A microkinetic model for catalytic ammonia synthesis over nonpromoted ruthenium is developed, based mostly on results from surface science investigations. Nitrogen dissociation is assumed to be the rate-determining step. In the preceding paper this process was investigated over an Ru(0001) surface, and it was found that only steps present in an amount of about 1% at the surface showed any significant activity. It is therefore assumed that only a small fraction of the surface sites on ruthenium catalysts are active, and for the nonpromoted catalysts a nitrogen dissociation rate equal to the rate at the steps of the Ru(0001) surface is used. The catalytic activities of an $Ru/MgAl_2O_4$ catalyst were measured for a wide range of conditions in order to thoroughly test the model. The model describes very well the activities of the $Ru/MgAl_2O_4$ catalyst as well as other experimental observations on ruthenium catalysts. As a result of fitting the observed negative reaction order for ammonia, the dominating nitrogen containing surface species is NH^*. This agrees well with the observed kinetic effects of promoting ruthenium with alkali metals which will interact repulsively with NH^*. The dominating surface species at low ammonia concentration is H^*, giving rise to the negative reaction order observed for hydrogen.

1. INTRODUCTION

Since the early pioneering work of Haber (1) on ammonia synthesis, it has been known that ruthenium catalysts exhibit high catalytic activities, and in the 1970s it was shown that catalysts based on ruthenium are better than iron-based catalysts under certain experimental conditions (2). Recently, there has been a renewed interest in ruthenium catalysts with the development of a very active multiple promoted carbon supported Ru catalyst and the resulting introduction of the Kellogg Advanced Ammonia Process (KAAP) (3). Currently, it is not known if the high cost and relative short lifetime of carbon-supported ruthenium catalysts compared to the traditional iron-based catalyst is justified by the increased activity.

Supports other than carbon have been used in the study of ruthenium catalysts; the most successful noncarbon support is MgO, especially when the catalyst is promoted with Cs (4, 5). The advantage of ruthenium catalysts, compared to the traditional multiple promoted iron catalyst, is that they are much less inhibited by ammonia, giving the possibility of operating at higher concentrations of ammonia (6).

Our understanding of ammonia synthesis over iron-based catalysts has been increased during the past decades both by applying new experimental techniques and by introducing advanced theoretical structure and energy calculations (7, 8). For the iron-based ammonia catalyst, surface science based microkinetic models have been successful in reproducing the observed catalytic activities and suggesting realistic reaction pathways (9–14).

In a study of the interaction of nitrogen with the Ru(0001) surface presented in the preceding paper (15, 16), it was found that the less than 1% atomic step sites inevitably present at the surface are totally dominating both the dissociation and the associative desorption of nitrogen. Experiments on supported ruthenium catalysts (17, 18) indicated that similar active sites are present at the surface of the small ruthenium particles of the supported catalysts. In the model only a small fraction of the sites on the ruthenium catalyst are therefore assumed to be active with a nitrogen dissociation rate equal to the rate measured over the steps at the Ru(0001) surface.

In order to test the microkinetic model, the catalytic activity of an $Ru/MgAl_2O_4$ catalyst has been determined under a wide range of process conditions. The $H_2:N_2$ ratio was varied between 6:1 and 1:4, the temperature was in the range 320–440°C, and the total pressure was between 1 and 100 bar. Based on these measurements activation energies and turnover frequencies were extracted and power-law kinetics were developed. This allows a comparison with previously published results from other research groups, and it is evident that the activity of the catalyst closely

0021-9517/00 $35.00

resembles the activity of the Ru/MgO catalyst investigated by Rosowski *et al.* (5).

For simplicity we have focused on nonpromoted samples where the surface science results are applicable, but based on the model the roles of promoters and the support are also discussed.

2. EXPERIMENTAL

The 11.1 wt% $Ru/MgAl_2O_4$ was prepared according to Fastrup (19) using a magnesium aluminum spinel carrier calcined at 1000°C with a BET surface area of 52 m^2/g and a pore radius of 13 nm determined by Hg intrusion.

The catalyst was activated in a flow of synthesis gas $H_2:N_2=3:1$ at 450°C for 20 h. The catalytic activities were determined in the multipurpose plug flow setup previously described (14), and 200 mg catalyst was tested using different gas mixtures of H_2 and N_2 in the temperature range 320 to 440°C and at pressures from 1 to 100 bar. The purity of the gas supply in the multipurpose unit was examined using the published procedure (20). After completion of the activity tests the catalyst was passivated in a stream of 1000 ppm O_2 in N_2.

Volumetric chemisorption of hydrogen was performed at room temperature in a commercial setup (Quantachrome), and the contribution from weakly physisorbed hydrogen was subtracted.

Transmission electron microscopy (TEM) was performed on the passivated catalyst to check the particle size distribution.

3. RESULTS

An H_2 monolayer capacity of 111 μmol/g was obtained from the volumetric chemisorption experiments. Assuming $H:Ru=1:1$ (21) the number of ruthenium surface atoms is 222 μmol/g. By a similar method Rosowski *et al.* (5) obtained a site density of 260 μmol/g for their Ru/MgO catalyst. However, their metal loading was only 5 wt% compared to 11.1 wt% Ru for our $Ru/MgAl_2O_4$ catalyst. Therefore, the calculated mean ruthenium particle size is 1.9 nm for their catalysts while it is 4.9 nm for our catalyst, assuming spherical particles. TEM micrographs of the $Ru/MgAl_2O_4$ catalyst show ruthenium particles ranging in size between 1 and 10 nm. Most abundant are particle sizes of about 1–3 nm, indicating that most of the active area of the catalyst stems from such small particles. TEM investigations of the Ru/MgO catalyst are consistent with a particle size of 2 nm (5).

All the activity data obtained for the $Ru/MgAl_2O_4$ catalyst are not listed here. Instead turnover frequencies (TOF) at selected conditions, reaction orders, and activation energies will be given. The full data set is available and can be obtained directly from the authors.

The determined site density is used to calculate the TOF from the activity measurements performed at a flow of 80 Nml/min over 200 mg catalyst. The results are compared in Table 1 with the TOF over 138 mg Ru/MgO catalyst at 40 Nml/min (5) using the same gas mixture ($H_2:N_2=3:1$).

For the $Ru/MgAl_2O_4$ catalyst, activation energies of 64 and 86 kJ/mol at 1 and 50 bar total pressure, respectively, were obtained at constant flow. The activation energies obtained for Ru/MgO are 69 and 78 kJ/mol at 1 and 20 bar total pressure, respectively, at constant flow (5).

The power law kinetics is derived from the activities obtained at 360°C since the most extensive data set is available at this temperature. The equation, activity $=kp_{N_2}^{\alpha}p_{H_2}^{\beta}p_{NH_3}^{\gamma}$, is fitted to the experimental data, varying k, α, β, and γ. The obtained parameters are compared to the similar data for Ru/MgO (5) in Table 2. The result $\alpha=1$ is in accordance with N_2 dissociation being the rate-determining step in ammonia synthesis.

All the preceeding results show that the $Ru/MgAl_2O_4$ and Ru/MgO catalysts are very similar with respect to TOF, temperature dependence, and reaction orders.

TABLE 2

Reaction Orders for the $Ru/MgAl_2O_4$ Catalyst and for the Ru/MgO Catalyst Characterized by Rosowski *et al.* (5)

Catalyst	P (bar)	T (K)	$\alpha(N_2)$	$\beta(H_2)$	$\gamma(NH_3)$
$Ru/MgAl_2O_4$	1–100	633	1.0	−0.5	−0.4
Ru/MgO	1	513–603	0.8	−0.3	−0.3
	20	573–663	1.0	−0.5	−0.3

TABLE 1

Turnover Frequencies (TOF) for the $Ru/MgAl_2O_4$ Catalyst and for the Ru/MgO Catalyst Investigated by Rosowski *et al.* (5)

Catalyst	P (bar)	588 K	593 K	623 K	633 K	673 K
$Ru/MgAl_2O_4$	1		7.2×10^{-4}		1.8×10^{-3}	3.3×10^{-3}
	50		1.1×10^{-3}		3.5×10^{-3}	8.5×10^{-3}
Ru/MgO	1	7.5×10^{-4}		1.6×10^{-3}		3.7×10^{-3}
	20	1.1×10^{-3}		3.0×10^{-3}		8.8×10^{-3}

4. MICROKINETIC MODEL

In this section the microkinetic model and how its parameters are obtained are described. Thereafter, the results of the model are presented.

The Reaction Mechanism

In the microkinetic model a reaction mechanism consisting of the following elementary reaction steps is assumed,

$$N_2 + 2* \rightleftharpoons 2N* \quad [1]$$

$$N* + H* \rightleftharpoons NH* + * \quad [2]$$

$$NH* + H* \rightleftharpoons NH_2* + * \quad [3]$$

$$NH_2* + H* \rightleftharpoons NH_3* + * \quad [4]$$

$$NH_3* \rightleftharpoons NH_3 + * \quad [5]$$

$$H_2 + 2* \rightleftharpoons 2H*, \quad [6]$$

where $*$ and X^* denote an empty site and a species X bonded to the surface, respectively. It is assumed that reaction [1] is the rate-determining step and that all the other reaction steps are in equilibrium. This is nearly the same mechanism as the one used in the model for ammonia synthesis over iron (9, 10), except that the adsorption of molecular nitrogen prior to dissociation is not considered. Adsorbed molecular nitrogen might well be a precursor for dissociation, but its low coverage under synthesis conditions makes it of no significance for the synthesis kinetics. Apart from this the same approximations as those of Stoltze and Nørskov (9, 10) are used, which basically means that interactions between the adsorbates, except for site blocking, are not considered. The expression for the synthesis rate per active site, r, is

$$r = 2k_1 p_{N_2} \theta_*^2 - 2k_{-1}\theta_N^2, \quad [7]$$

where k_1 and k_{-1} are the forward and backward rate constants for reaction [1], respectively, and θ_* and θ_N are the coverage of free sites and of N*, respectively. The coverages are given relative to the number of ruthenium surface atoms, which is equal to the number derived from hydrogen chemisorption (21).

The saturation coverage of nitrogen at the Ru(0001) surface is approximately 1/3 of a monolayer (ML) (22), and for hydrogen it is 1 ML (23). On the Ru(10$\bar{1}$0) surface the ratio between the saturation coverage of nitrogen and hydrogen is nearly the same (24, 25). When dissociating N_2 at the Ru(0001) surface a nitrogen coverage of 1/4 ML could only be achieved [15], but the more relevant coverage at the steps is not known and might be higher. Considering the difference in saturation coverage, there is no obvious way to describe how hydrogen blocks the free sites avaliable for nitrogen dissociation, and therefore two approaches are tested. In the first it is assumed that

$$\theta_* = 1 - 3\theta_{NH_x} - \theta_H, \quad [8]$$

which corresponds to less blocking of surface sites by hydrogen than by nitrogen-containing surface species (NH_x, $x = 0$–3). This approach results in the correct saturation coverage of both nitrogen and hydrogen when the number of sites is equal to the number of Ru surface atoms involved. In the second approach, equal blocking by all the surface species is assumed; i.e.,

$$\theta_* = 1 - 3\theta_{NH_x} - 3\theta_H. \quad [9]$$

The normally used expression, where one adsorbate blocks one site, could equally well have been used here if the number of active sites was reduced by a factor of three. This would, however, require that the rate and equilibrium constants be changed according to the reduction in the number of active sites, which would increase the coverage values involved in the rate and equilibrium expressions by a factor of three.

In the work on nitrogen adsorption on the Ru(0001) surface (15) it was found that about 1% of step sites gave rise to a sticking coefficient of $s_0 = 10^{-5.4}\exp(-36\ \text{kJ mol}^{-1}\ R^{-1}\ T^{-1})$ for the whole surface. The sticking coefficient at the active step sites is therefore about 100 times higher than this value. Only part of the surface of a ruthenium catalyst is considered to have active sites with an activity equal to the one of the step sites on the Ru(0001) surface. In the microkinetic model it is assumed that this part of the surface is dissociating all the N_2, and the rest of the surface is considered to have negligible activity. These sites are therefore determining the ammonia synthesis rate, and it is of no importance that reactions [2] to [6] might also take place at other parts of the surface.

From the flux of nitrogen molecules hitting the surface and a site density equal to the atom density on the Ru(0001) surface, the following dissociation rate constant for the active sites is found:

$$k_1 = \frac{1.2 \times 10^6\ \text{bar}^{-1}\ K^{0.5}\ \text{s}^{-1}}{\sqrt{T}} \exp\left(\frac{-36\ \text{kJ/mol}}{RT}\right). \quad [10]$$

Equilibrium Constants

To obtain the equilibrium constants for reactions [2] to [6], statistical mechanics is used as described by Stoltze (10). The parameters needed are the energies, vibration frequencies, and rotational constants for all the different species involved. The data for the gas-phase molecules are well known (11). In Table 3, the measured vibration frequencies for surface species adsorbed at well-defined single-crystal surfaces of ruthenium are presented. In the preceding paper (15) it was argued that both the Ru(10$\bar{1}$0) and the Ru(11$\bar{2}$1) faces have sites whose geometry resembles that of the active

TABLE 3

Measured Vibration Frequencies (cm^{-1}) for the Different Surface Species on Ruthenium

N^{*a}	NH^{*b}	NH_2^{*b}	NH_3^{*b}	H^{*c}
331(2)	694	516	121(2)	282(2)
484	1314(2)	1524	355	847
	3315	3290	565(2)	
		3379	1129	
			1564(2)	
			3242	
			3379(2)	

Note. The data are obtained by measurements on the Ru(10$\bar{1}$0) or the Ru(11$\bar{2}$1) surfaces. The frequencies that are taken to be doubly degenerate are followed by (2).

[a] Reference (24).

[b] Reference (26).

[c] Reference (25).

step sites on the Ru(0001) surface. Therefore, data measured on these surfaces are used when available in the literature. However, the vibration frequencies of the adsorbed species are not very dependent on the surface structure (26), and it is of minor importance which surface is used.

By necessity some of the constants have to be estimated since they have not been measured. Consequently, 201 and 194 cm^{-1} are used for the rotation constants of NH_2^* and NH_3^*, respectively, which are the values similarly applied by Stoltze on iron (11). The frequencies used for the frustrated translations parallel to the surface of NH^* and NH_2^* are 261 and 191 cm^{-1}, respectively, which are between the measured frequencies for NH_3^* and N^*. For the two frustrated rotations of NH_2^* a single value of 940 cm^{-1} is used which is the average of the values used for NH_3^* and NH^*.

The energies at 0 K for the different surface species also have to be determined. They are normally different from the adsorption enthalpies obtained at higher temperatures. Here the energy values relative to the energies of the gas-phase molecules N_2 and H_2 are given, including the zero point energies.

An isosteric heat of adsorption of 82 kJ/mol was obtained for H_2 adsorption on the Ru(10$\bar{1}$0) surface up to a coverage of 0.5 ML (25). This adsorption enthalpy is obtained at 400°C using an energy of −41.5 kJ/mol for H^*.

To find a value for the adsorption energy of NH_3^* the tailing edge of NH_3–TPD spectra from the Ru(0001) surface (27–29) is fitted, assuming first-order desorption. The tailing edge is used since this part most probably originates from NH_3 desorption from the steps of the surface. Ammonia decomposes before desorption at the more open ruthenium surfaces, and therefore no NH_3–TPD spectra are available. In order to obtain an adsorption energy from the TPD spectrum the sticking coefficient for NH_3 on the Ru(0001) is assumed to be 0.2, as was found experimentally (27). The adsorption energy for NH_3^* is then estimated to be 105 kJ/mol, and the energy of NH_3^* becomes −143.6 kJ/mol.

It was found that an activation barrier of 145 kJ/mol and a preexponential factor of 10^{-12} s^{-1} for desorption from the steps at the Ru(0001) surface could describe the desorption of nitrogen from this surface (15). From the relation

$$K_1 = \frac{k_1}{k_{-1}} \qquad [11]$$

a desorption rate for nitrogen close to this rate is obtained by using an energy for N^* of $^*-57$ kJ/mol.

The energies of NH^* and NH_2^* are as first approximations chosen to be −85.9 and −114.7 kJ/mol, respectively, evenly spaced between the energies of N^* and NH_3^*. This might not be a good approach since it has been shown that both NH^* and NH_2^* are quite stable on ruthenium surfaces (24, 26, 30), and most often NH^* is found to be the most stable of the two (24). This stability is apparently not due to high decomposition barriers since it has been possible to synthesize ammonia from preadsorbed nitrogen and hydrogen at room temperature both on the Ru(0001) surface (30) and the Ru(10$\bar{1}$0) surface (24). Likewise, on ruthenium powder it has been reported that hydrogenation of preadsorbed nitrogen to ammonia is possible at temperatures as low as −70°C (31). Using the proposed energies for NH^* and NH_2^* results in N^* and H^* being the energetically stable form of nitrogen and hydrogen on the surface.

Using the Model

Most of the parameters needed in the microkinetic model have now been determined as discussed above. However, in order to quantify the fraction of empty sites, a decision between Eqs. [8] and [9] has to be made, and also the energies of NH^* and NH_2^* might have to be changed. First the model is used to predict the synthesis rates obtained over an Ru single crystal in a microreactor with a constant gas flow. The reactor is a continously stirred tank reactor (CSTR) (32). It is possible to achieve good agreement between the model and the experiments by using both Eqs. [8] and [9] to describe the site blocking. Equation [8] gives the best result if the number of active sites, which is a fitting parameter, is less than 1.5% of the total number of surface atoms. This is not realistic since the reaction occurred both at the Ru(0001) surface which was miscut by 4° as and at the rim of the crystal (32). The step density should therefore be much higher than on the well-aligned Ru(0001) surface where a step density of 1% was used when determining the N_2 dissociation rate. Hence, Eq. [9] is chosen to describe the number of free sites and thereby the inhibition by hydrogen. The agreement between the experiment and the model when using a step density of 9% is shown in Fig. 1. Lowering the energies for NH^* and NH_2^* gave no significant difference in the performance of the model due to the

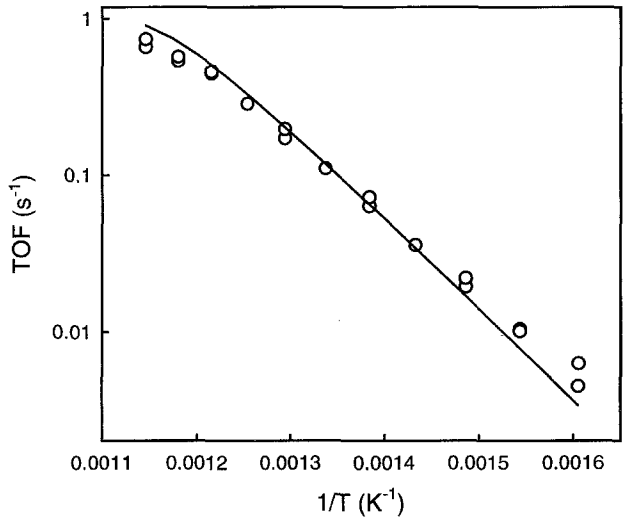

FIG. 1. Turnover frequency of the ammonia synthesis reaction over a ruthenium single crystal versus the inverse temperature. The open circles are the measures values, and the full line is the result of the model when using the same conditions and assuming that only 9% of the surface sites are active. The turnover frequencies are determined relative to the total number of surface atoms/sites.

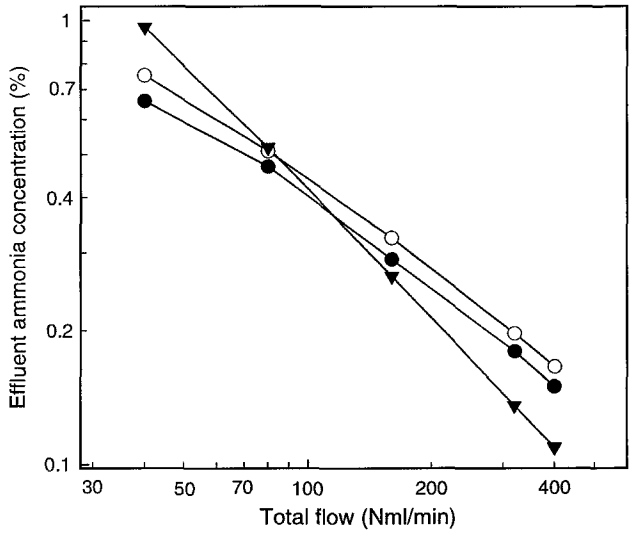

FIG. 2. Effluent ammonia concentration from a plug flow reactor as a function of gas flow using an $H_2 : N_2$ ratio of 1 : 1, a total pressure of 50 bar, and a temperature of 360°C. The filled circles are the experimental results using 200 mg catalyst. The filled triangles are the results of the microkinetic model using energies of NH^* and NH_2^* between the energies of N^* and NH_3^*, and an active site density of 10 μmol/g. The open circles display the outcome of the microkinetic model when the energy of NH^* is decreased by 22.5 kJ/mol, the energy of NH_2^* is decreased by 11.3 kJ/mol, and the active site density is 20 μmol/g.

low ammonia partial pressures in the experiments. These experiments are therefore not suitable for estimating the energies of NH^* and NH_2^*.

It is seen in Fig. 1 that the model results in an apparent activation energy which is too high compared to that of the experiments. There are two ways to correct this; one is to decrease the activation barrier for N_2 dissociation, and the other is to decrease the adsorption energy of hydrogen. Both will result in fewer active sites being needed, which is contrary to our knowledge of the single-crystal surface, as described above.

The reactor where the reaction rates over the Ru/$MgAl_2O_4$ catalyst were obtained is represented in the model by an ideal plug flow reactor. In such a reactor any diffusion effects are neglected. Numerically, this type of reactor is treated by dividing it into a number of reactors along the flow direction and treating each of these as a CSTR. The number of reactors chosen is large enough that the relative change in reaction rate between consecutive reactors is small. Using the approximation given above for the energies of NH^* and NH_2^* results in an exit ammonia concentration dependence of the gas flow, which is far from what is seen experimentally, as shown in Fig. 2. In order to achieve satisfactory agreement with the experimental observations, the energy of NH^* was lowered to −108.4 kJ/mol and the energy of NH_2^* was set to the average of the energies of NH^* and NH_3^*. The results are displayed in Fig. 2. This makes NH^* the energetically stable form of nitrogen and hydrogen on the surface as was suggested by the surface science observations. The high stability of NH^* has recently been confirmed by DFT calculations (33).

Except for the number of active sites, all the parameters in the microkinetic model have now been fixed, and Fig. 3 illustrates the ability of the model to describe the performance of the Ru/$MgAl_2O_4$ catalyst under all the different

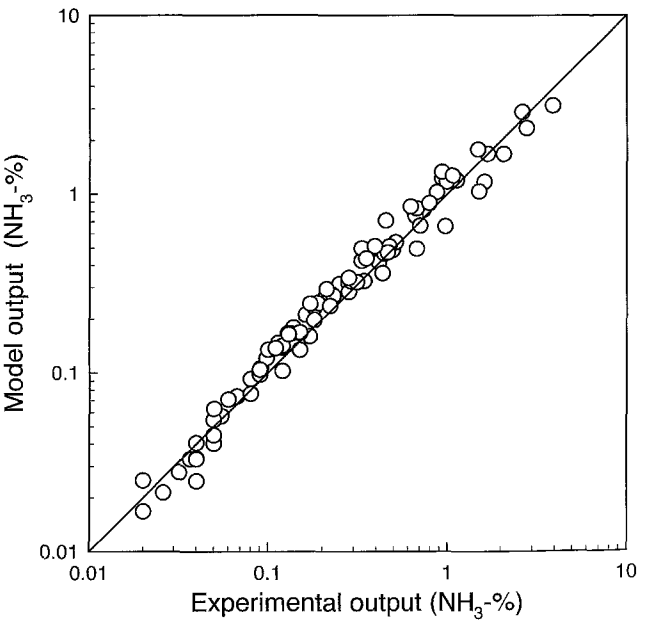

FIG. 3. Comparison between measured and calculated NH_3 production for the Ru/$MgAl_2O_4$ catalyst: pressure, 1–100 bar; $H_2 : N_2$ ratio, 6 : 1–1 : 4; temperature, 320–440°C.

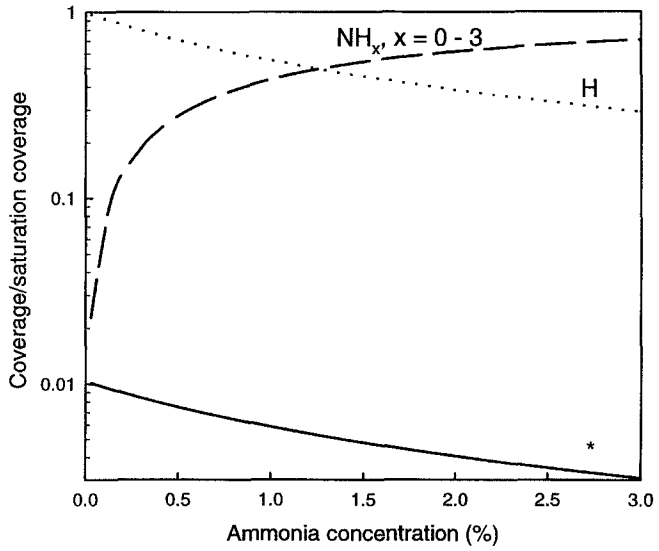

FIG. 4. The coverages of *, NH_x^*, and H* as a function of ammonia concentration when the total pressure is 50 bar, the temperature is 400°C, and the $H_2:N_2$ ratio is 3:1. The coverages are taken relative to the saturation coverages of the different species. The ratio between the coverages of $N^*:NH_3^*:NH_2^*:NH^*$ is approximately 1:1:10:50 at all ammonia concentrations.

conditions used for testing. The model predicts all the measured outlet concentrations of ammonia at better than a factor 1.6 when using an active site density of 20 μmol/g. This is 9% of the number of surface atoms measured with hydrogen chemisorption.

The fractional coverage of surface species at the active sites during synthesis as a function of ammonia concentration is shown in Fig. 4, for when the total pressure is 50 bar, the temperature is 400°C, and the $H_2:N_2$ ratio is 3:1. All the coverages are taken relative to the saturation coverage of each species.

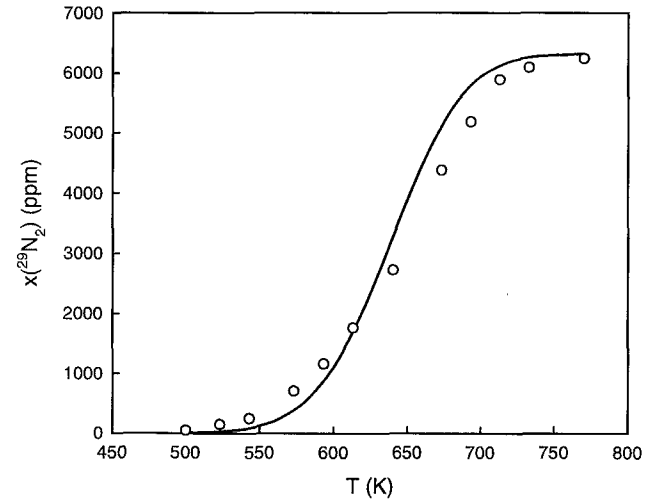

FIG. 5. The full line is the calculated outlet concentration of $^{29}N_2$ when an inert gas containing 0.67% $^{28}N_2$ and 0.60% $^{30}N_2$ is passed over 138 mg of catalyst containing 20 μmol/g active sites. The flow is 50 Nml/min and the reactor is treated as a plug flow reactor. The conditions are equal to the ones used by Hinrichsen *et al.* (18) over the Ru/MgO catalyst and the open circles are their results.

TABLE 4

Preexponential Factors and Activation/Reaction Enthalpies for the Rate Constants/Equilibrium Constants Used in the Microkinetic Model for Ammonia Synthesis over Nonpromoted Ru

Constant	Preexponential factor	Activation energy/ reaction enthalpy
k_1	2.8×10^4 bar^{-1} s^{-1}	33 kJ/mol
k_{-1}	2.9×10^{12} s^{-1}	145 kJ/mol
K_2	5.3×10^{-2}	−18 kJ/mol
K_3	0.82	20 kJ/mol
K_4	0.26	20 kJ/mol
K_5	2.8×10^7 bar	106 kJ/mol
K_6	1.2×10^{-5} bar^{-1}	−82 kJ/mol

Note. The constants were determined at 400°C.

The turnover frequencies and reaction orders show that the $Ru/MgAl_2O_4$ catalyst closely resembles the Ru/MgO catalyst synthesized and characterized by Muhler and Ertl's group (5, 17, 18). It is therefore not surprising that the synthesis rates reported for the Ru/MgO catalyst can be described well by the microkinetic model if the active site density is also set to 20 μmol/g, which is equal to 8% of the number of sites on the Ru/MgO catalyst as measured with hydrogen chemisorption (5). The Ru/MgO catalyst was also used in nitrogen isotope exchange experiments where a mixture of $^{28}N_2$ and $^{30}N_2$ was passed over the catalyst at different temperatures after which the $^{29}N_2$ concentration was measured (18). By using the active site density of 20 μmol/g, the microkinetic model simulates these results well, as seen in Fig. 5.

In order to present the model in a more transparent form all the rate constants and equilibrium constants are given in Arrhenius form, by preexponential factors and activation/reaction enthalpies, in Table 4. These parameters depend on temperature and are determined at 400°C, which is a common synthesis temperature.

5. DISCUSSION

The microkinetic model that is presented has been developed for ammonia synthesis over nonpromoted ruthenium catalysts. It describes very well the synthesis rates of ammonia over a ruthenium single crystal (Fig. 1) and over an $Ru/MgAl_2O_4$ catalyst (Figs. 2 and 3). The model is to a large extent based on surface science results for the relevant surface species on ruthenium. However, some "fitting" has also been performed in order to obtain parameters that are not available from direct measurements. The model is also in

excellent agreement with an N_2 isotope scrambling experiment over an Ru/MgO catalyst (Fig. 5). The latter result clearly indicates that the values of k_1 and k_{-1}, obtained from the surface science experiments, correctly describe the dissociation and desorption of nitrogen at the surface of small ruthenium particles.

The fact that the model is in good agreement with many widely different experimental results strongly suggests that it gives a fundamentally correct picture of ammonia synthesis over ruthenium. Therefore, it is relevant to discuss the results and the parameters of the model.

The Number of Active Sites

Both for the single crystal and the $Ru/MgAl_2O_4$ catalyst, an active site density corresponding to about 9% of the site density obtained by H_2 chemisorption was used. A minimum of 7% of step sites are present on the 4° miscut Ru(0001) surface; therefore, 9% is a reasonable number of active sites since there is probably a high number of step sites on the rim of the crystal which was also active in the experiments (32).

Density functional calculations have shown that there are two reasons for the low dissociation barrier at the step on the Ru(0001) surface (16). The first and most important is the geometry of the site, which allows five surface atoms to be part of the transition state complex instead of four on the flat terrace. The second is the low coordination and therefore generally higher reactivity of the step atoms (34). The atoms with low coordination number on small Ru particles are edge atoms. The number of edge atoms depends on the particle shape, but a 2-nm particle will generally have edge atoms amounting to approximately 40% of the surface atoms, and a 4-nm particle will have approximately 20% (35). Many of these edge atoms are not part of sites with the correct geometry for low-barrier nitrogen dissociation, and it is therefore consistent that a lower number of the surface sites (atoms) were found to be active on the supported catalyst.

Rosowski *et al.* (17) and Hinrichsen *et al.* (18) also concluded that only a small fraction of the sites on the Ru/MgO catalyst were active, and they attributed this to electronic promotion by oxygen vacancies of the support. This possibility cannot be rejected, but the present work suggests that the active sites of the Ru/MgO catalyst only need the activity observed at step sites of the Ru(0001) surface where no promotion is present. If promotion or poisoning by the support is ruled out, then different morphologies of the ruthenium particles is the only explanation for the observed strong support dependence of the ammonia synthesis activity (4, 5, 18).

The investigations of nitrogen dissociation over the Ru(0001) surface (15) show that ammonia synthesis over ruthenium is a very structure-sensitive reaction if the N_2 dissociation is rate determining. For supported catalysts an activity dependence on particle size is considered to be a sign of structure sensitivity (36), and if the number of edge atoms with low coordination number is important for the number of active sites, then one would expect small ruthenium particles to be relatively more active than big ones.

Kowalczyk *et al.* have recently investigated the effect of particle size on the activity of a Ba-promoted Ru/C catalyst (37), and they saw no influence of particle size on the activity per surface atom. Though this is in conflict with the hypothesis given above, it can be argued that the electronic promotion by Ba reduces the importance of the number of low coordinated step atoms. The particle size dependence has also been investigated over Ru particles supported on zeolites; increasing catalytic activity with increasing particle size was found in two cases (38, 39), and no dependence, was found in one case [40].

In this discussion it is important to note that the *geometry* of the active site is more important than a low coordination number (16), and the fraction of sites with the *right* geometry might decrease when the particle size is decreased. It is therefore not certain that any activity dependence on particle size can be observed for ammonia synthesis over supported Ru catalyst, even though the reaction is strongly structure sensitive. These geometric aspects of structure sensitivity have been discussed by Bennett *et al.* (41), and the conclusion is that combinations of geometric effects, electronic effects, and support effects can produce any kind of activity dependence on particle size.

The Coverage of Surface Species During Synthesis

According to our microkinetic model, the active sites are mostly blocked by hydrogen when the NH_3 concentration is low. When the NH_3 concentration gets higher the surface is more blocked by nitrogen-containing surface species. An example of this is seen in Fig. 4. The reaction orders are determined, according to Stoltze (10), by the surface composition: A high coverage of nitrogen-containing species, which are in equilibrium with ammonia in the gas phase, results in a negative reaction order for ammonia, and a high coverage of hydrogen results in a negative reaction order for hydrogen. The coverages obtained in the model are therefore consistent with the fact that the reaction orders for both hydrogen and ammonia are negative; see Table 2. The ratio of the coverages of the nitrogen-containing species is approximately $\theta_N : \theta_{NH_3} : \theta_{NH_2} : \theta_{NH} = 1 : 1 : 10 : 50$. The dominant NH^* is known to posses a dipole moment on ruthenium (42) and neighboring NH^* species will therefore interact repulsively; hence the approximation of noninteracting surface species might be invalid. On the other hand, the few active sites are perhaps sufficiently separated in space that the approximation is still good. As described above, the energy of NH^* was chosen such that the observed inhibition of ammonia could be accounted for. As the reaction order of NH_3 is determined by the coverage of nitrogen-containing

species this would also be achieved by decreasing the energy of one or more of the other nitrogen-containing species. It is not consistent with the surface science experiments to decrease the energy of N* and/or NH_3^*. However, it has been shown that N* and NH* can stabilize each other on Ru(0001) (42), as well as N* and NH_3^* (28), indicating a decrease in energies for all the different nitrogen-containing species on the ruthenium catalyst surface under operating conditions. We have not tried to work with such an effect in our model, but it would most certainly have a similar effect on the kinetics as the decreased energy of NH* used here.

Possible Effects of Electronic Promoters

When alkali metal promoters like K and Cs are added to ruthenium catalysts for ammonia synthesis, this normally results in four observable changes: (1) the catalyst becomes much more active, (2) the reaction order of ammonia changes from negative to about zero, (3) the reaction order for hydrogen decreases and can get close to -1, and (4) the apparent activation energy measured at constant flow is increased (4, 5).

It is well known that alkali metals adsorbed on a metal surface donate negative charge to the surface. Since NH* adsorbed on ruthenium does the same (42), it is destabilized by alkali metals.

Theoretical calculations have shown that the presence of alkali metal on the Ru(0001) surface lowers the barrier for N_2 dissociation through a direct electrostatic interaction (8), which is confirmed by the higher isotope exchange rate over a Cs-promoted Ru/MgO catalyst compared to the nonpromoted catalyst (18).

Based on the present model, these effects of alkali metal promotion will change the kinetics in the directions observed. The rate will increase due to the higher dissociation rate and less inhibition by NH*, and the reaction order for ammonia will increase as an effect of the latter. The reaction order for hydrogen will decrease to about -1 since hydrogen will totally dominate the surface when there is little NH* and other nitrogen-containing surface species. The increase in apparent activation energy for ammonia synthesis when promoting with alkali metal is also captured by the model solely by increasing the energies of the NH_x^* ($x = 1$–3) species. NH_3^* is also shown to be destabilized by alkali metals (29), and we assume the same for NH_2^*. If the energy of all these species is increased by, for instance, 30 kJ/mol the microkinetic model predicts an 18 kJ/mol increase in the apparent activation energy at constant flow. This increase is mainly due to the decrease in ammonia inhibition. Hinrichsen *et al.* (43) have made a microkinetic model for a Cs-promoted Ru/MgO catalyst using the same reaction mechanism as that used in this study. Comparing the parameters of the two models, it is evident that the main differences are precisely their higher energies for the NH_x, $x = 1$–3, species compared to ours.

The model can qualitatively explain all the changes observed when ruthenium catalysts are promoted with alkali metal due to the rather high coverage of NH_x, $x = 1$–3, during synthesis over the nonpromoted catalysts. The same effect would not be anticipated if the surface was dominated by N* since it possesses an opposite dipole moment compared with NH* (42). Based on single-crystal investigations, destabilization of NH_3^* and increased N_2 dissociation rate have also been proposed to explain the promotion of ammonia synthesis over iron by K (44, 45).

Comparison to Microkinetic Model for Iron

The microkinetic model by Stoltze and Nørskov for ammonia synthesis over iron predicts a surface dominated by N* under most conditions (10). This is due to a higher adsorption energy of N* on iron than on ruthenium (91 kJ/mol per N* on iron (11) and 57 kJ/mol on ruthenium), and it is the reason that ruthenium can be a better catalyst for ammonia synthesis than iron, even though the N_2 dissociation rate on ruthenium is lower than on iron. The condition that favors ammonia synthesis over Ru compared to Fe is a high partial pressure of ammonia, particularly when the catalyst is promoted with alkali metal.

The Reaction Mechanism

There are other possible reaction mechanisms for ammonia synthesis than the one used here. One is that adsorbed N_2 is hydrogenated before it dissociates, and such a mechanism has recently been found to prevail in ammonia synthesis by the enzyme nitrogenase (46). This was also proposed for the $Ru/MgAl_2O_4$ catalyst (19), but the present results favor the mechanism discussed here as the proper one at ruthenium metal surfaces, in particular because of the fact that the model can account for both the N_2 isotope scrambling experiment over the Ru/MgO catalyst (Fig. 5) and the ammonia synthesis activities (Figs. 1 and 3.)

6. CONCLUSIONS

A microkinetic model for ammonia synthesis over nonpromoted ruthenium which is based predominantly on surface science observations has been developed. The main input to the model is the rate-determining N_2 dissociation rate, measured at the steps of an Ru(0001) surface, which is the only part of the surface that is active in the reaction. The model describes very well the synthesis rates measured over a ruthenium single crystal and the rates obtained over an $Ru/MgAl_2O_4$ catalyst for a wide range of synthesis conditions. The model was also able to describe an N_2 isotope exchange experiment over a nonpromoted Ru/MgO catalyst. To obtain satisfactory agreement with the experimental results it was necessary to fit the energy of NH*. This resulted in surface coverages during synthesis which are consistent with the change in kinetics when the ruthenium

catalyst is promoted with alkali metal. Given the success of the model for describing widely different experiments, we are confident that it contains the main features of ammonia synthesis over ruthenium and particularly that the reaction mechanism is correct.

ACKNOWLEDGMENTS

Discussions with and suggestions from J. K. Nørskov are gratefully acknowledged. The present work was in part financed by The Danish Research Councils through grant 9501775. The Center for Atomic-Scale Materials Physics (CAMP) is sponsored by the Danish National Research Foundation.

REFERENCES

1. Mittasch, A., *Adv. Catal.* **2**, 81 (1950).
2. Aika, K.-I., Hori, H., and Ozaki, A., *J. Catal.* **27**, 424 (1972).
3. U.S. Patent 4,163,775 (1979); U.S. Patent 4,568,532 (1984); U.S. Patent 4,479,925 (1984).
4. Aika, K.-I., and Tamaru, K., *in* "Ammonia: Catalysis and Manufacture" (A. Nielsen, Ed.), p. 103. Springer-Verlag, Berlin/New York, 1995.
5. Rosowski, F., Hornung, A., Hinrichsen, O., Herein, D., Muhler, M., and Ertl, G., *Appl. Catal. A Gen.* **151**, 443 (1997).
6. Kowalczyk, Z., Jodzis, S., and Sentek, J., *Appl. Catal. A Gen.* **138**, 83 (1996).
7. Mortensen, J. J., Gandublia-Pirovana, M. V., Hansen, L. B., Hammer, B., and Nørskov, J. K., *Surf. Sci.* **422**, 8 (1999); Mortensen, J. J., Hansen, L. B., Hammer, B., and Nørskov, J. K., *J. Catal.* **182**, 479 (1999).
8. Mortensen, J. J., Hammer, B., and Nørskov, J. K., *Phys. Rev. Lett.* **80**, 4333 (1998); *Surf. Sci.* **414**, 315 (1998).
9. Stoltze, P., and Nørskov, J. K., *Phys. Rev. Lett.* **55**, 2502 (1985).
10. Stoltze, P., *Phys. Scripta* **36**, 824 (1987).
11. Stoltze, P., and Nørskov, J. K., *Topics Catal.* **1**, 253 (1994).
12. Bowker, M., *Catal. Today* **12**, 153 (1992).
13. Fastrup, B., *Topics Catal.* **1**, 273 (1994).
14. Sehested, J., Jacobsen, C. J. H., Törnqvist, E., Rokni, S., and Stoltze, P., *J. Catal.* **188**, 83 (1999).
15. Dahl, S., Törnqvist, E., and Chorkendorff, I., *J. Catal.* **192**, 381 (2000).
16. Dahl, S., Logadottir, A., Egeberg, R. C., Larsen, J. H., Chorkendorff, I., Törnqvist, E., and Nørskov, J. K., *Phys. Rev. Lett.* **83**, 1814 (1999).
17. Rosowski, F., Hinrichsen, O., Muhler, M., and Ertl, G., *Catal. Lett.* **36**, 229 (1996).
18. Hinrichsen, O., Rosowski, F., Hornung, A., Muhler, M., and Ertl, G., *J. Catal.* **165**, 33 (1997).
19. Fastrup, B., *Catal. Lett.* **48**, 111 (1997).
20. Fastrup, B., and Nielsen, H. N., *Catal. Lett.* **14**, 233 (1992).
21. Dalla Betta, R. A., *J. Catal.* **34**, 57 (1974).
22. Dietrich, H., Jacobi, K., and Ertl, G., *J. Chem. Phys.* **105**, 8944 (1996).
23. Shi, H., and Jacobi, K., *Surf. Sci.* **313**, 289 (1994).
24. Dietrich, H., Jacobi, K., and Ertl, G., *J. Chem. Phys.* **106**, 9313 (1997).
25. Lauth, G., Schwarz, E., and Christmann, K., *J. Chem. Phys.* **91**, 3729 (1989).
26. Dietrich, H., Jacobi, K., and Ertl, G., *Surf. Sci.* **352–354**, 138 (1996).
27. Dannielson, L. R., Dresser, M. J., Donaldson, E. E., and Dickingson, J. T., *Surf. Sci.* **71**, 599 (1978).
28. Sun, Y.-K., Wang, Y.-Q., Mullins, C. B., and Weinberg, W. H., *Langmuir* **7**, 1689 (1991).
29. Bennedorf, C., and Madey, T. E., *Surf. Sci.* **135**, 164 (1983).
30. Shi, H., Jacobi, K., and Ertl, G., *J. Chem. Phys.* **102**, 1432 (1995).
31. Rambeau, G., and Amariglio, H., *J. Catal.* **72**, 1 (1981).
32. Dahl, S., Taylor, P. A., Törnqvist, E., and Chorkendorff, I., *J. Catal.* **178**, 679 (1998).
33. Rod, T. H., Logadottir, A., and Nørskov, J. K., *J. Chem. Phys.* **112**, 5343 (2000).
34. Hammer, B., Nielsen, O. H., and Nørskov, J. K., *Catal. Lett.* **46**, 31 (1997).
35. Duke, C. B., and Tucker, C. W., Jr., *Surf. Sci.* **15**, 231 (1969).
36. Boudart, M., *Adv. Catal. Realt. Subj.* **20**, 153 (1969).
37. Kowalczyk, Z., Jodzis, S., Raróg, W., Zieliński, J., Pielaszek, J., and Presz, A., *Appl. Catal. A Gen.* **184**, 95 (1999).
38. Guntow, U., Rosowski, F., Muhler, M., Ertl, G., and Schlögl, R., *Stud. Surf. Sci. Catal.* **91**, 217 (1995).
39. Cisneros, M. D., and Lunsford, J. H., *J. Catal.* **141**, 191 (1993).
40. Wellenbüscher, J., Rosowski, F., Klengler, U., Muhler, M., Ertl, G., Guntow, U., and Schlögl, R., *Stud. Surf. Sci. Catal.* **84**, 941 (1994).
41. Bennett, C. O., and Che, M., *J. Catal.* **120**, 293 (1989).
42. Dietrich, H., Jacobi, K., and Ertl, G., *Surf. Sci.* **377–379**, 308 (1997).
43. Hinrichsen, O., Rosowski, F., Muhler, M., and Ertl, G., *Chem. Eng. Sci.* **51**, 1683 (1996).
44. Strongin D. R., and Somorjai G. A., *in* "Catalytic Ammonia Synthesis Fundamentals and Practice" (J. R. Jennings, Ed.), p. 133. Plenum, New York, 1991.
45. Ertl, G., *in* "Catalytic Ammonia Synthesis Fundamentals and Practice" (J. R. Jennings, Ed.), p. 109. Plenum, New York, 1991.
46. Rod, T. H., Hammer, B., and Nørskov, J. K., *Phys. Rev. Lett.* **82**, 4054 (1999).